HHS Public Access

Author manuscript

Phytochemistry. Author manuscript; available in PMC 2022 January 01.

Published in final edited form as:

Phytochemistry. 2021 January ; 181: 112545. doi:10.1016/j.phytochem.2020.112545.

Antibacterial kaneoheoic acids A-F from a Hawaiian fungus *Fusarium* sp. FM701

KH Ahammad Uz Zaman[a], **Xiaohua Wu**[a], **Zhenquan Hu**[b,c], **Wesley Yoshida**[d], **Shaobin Hou**[e], **Jennifer Saito**[e], **Kristiana Alexes Avad**[f], **Kirk E. Hevener**[f], **John N. Alumasa**[g], **Shugeng Cao**[a,h,*]

[a]Department of Pharmaceutical Sciences, Daniel K. Inouye College of Pharmacy, University of Hawai'i at Hilo, Hilo, HI, 96720, United States

[b]Warshel Institute for Computational Biology, The Chinese University of Hong Kong, Shenzhen, People's Republic of China

[c]School of Chemistry and Materials Science, University of Science and Technology of China, People's Republic of China

[d]Department of Chemistry, University of Hawai'i at Manoa, Hawaii, United States

[e]Advanced Studies in Genomics, Proteomics and Bioinformatics (ASGPB), University of Hawai'i at Manoa, Honolulu, HI, 96822, United States

[f]College of Pharmacy, University of Tennessee Health Science Center, United States

[g]Department of Biochemistry and Molecular Biology, Pennsylvania State University, United States

[h]Cancer Biology Program, University of Hawaii Cancer Center, 701 Ilalo Street, Honolulu, Hawai'i, 96813, United States

Abstract

Alarming rate of resistance to the existing antibiotics exhibits the importance of developing new antibiotic molecules from relatively under explored sources as well as implementing alternative approaches like antibiotic adjuvants. Six previously undescribed fungal polyketides, kaneoheoic acids A-F (**1–6**) were isolated from a fungal strain *Fusarium* sp. FM701 which was collected from a muddy sample of Hawaiian beach. The structures of these six compounds were elucidated by spectroscopic interpretation, including HRESIMS and NMR, and electronic circular dichroism (ECD) analysis. All six compounds that were inactive when tested alone showed significant antibacterial activity against *Staphylococcus aureus* and *Bacillus subtilis*, in the range of 10–80 μg/mL when assayed in combination with either chloramphenicol (half of the MIC, 1 μg/mL), an FDA approved antibiotic or disulfiram (6 μg/mL), an established antibiotic adjuvant that augmented the activity of antibiotics.

*Corresponding author. Department of Pharmaceutical Sciences, Daniel K. Inouye College of Pharmacy, University of Hawai'i at Hilo, Hilo, HI, 96720, United States. scao@hawaii.edu (S. Cao).

Declaration of competing interest

The authors declare that they have no known competing financial interests or personal relationships that could have appeared to influence the work reported in this paper.

Keywords

Hawaiian fungi; *Fusarium sp.*; polyketides; Antibacterial activity; Disulfiram

1. Introduction

Due to rapid growth of population and growing resistance to existing anti-biotic drugs, there is a need for the development of new antibiotics from relatively new natural sources. One approach is to uncover new biologically active molecules from unique ecological niches, which have the potential to be developed further into drugs. Fungi, as a rich source, produce a huge number of biologically active secondary metabolites, including a wide variety of clinically significant drugs. For example, fungi play a vital role in the production of beta-lactam antibiotics like penicillin and cephalosporin, as well as the immunosuppressant cyclosporine and cholesterol lowering agents, compactin and lovastatin [Aly et al., 2011; Manzoni and Rollini, 2002]. Considering the biodiversity of the fungal kingdom and the fact that only a small fraction of fungi has ever been explored for the secondary metabolites with biological activity, it is obvious that a variety of biologically active compounds are still to be discovered. Located in the central Pacific Ocean, Hawaii has its own ecosystems with a unique biodiversity and fungi play a vital role in this system. In our continuing search for biologically active compounds from Hawaiian fungi [Zaman et al., 2020; Wang et al., 2019a, Wang et al., 2020; Li et al., 2019, 2018; Fei-Zhang et al., 2016; Huang et al., 2017], we isolated a fungus *Fusarium* sp. FM701 (Genbank accession # MW130722) from a muddy sample collected at the Kaneohe Bay, Oahu, Hawaii. *Fusarium* species is well-known to produce mycotoxins such as fumonisins, fusaric acid, trichothecenes, fusaproliferin, moniliformin, and enniatins, with unique structures including polyketides, alkaloids, and terpenoids [Fotso et al., 2002]. These types of compounds are interesting due to broad-spectrum of biological properties, for example, antifungal, antibacterial, insecticidal, and cytotoxic activities [Song et al., 2015]. Recently, a crude methanolic extract of *Fusarium* sp. FM701, which was not active by itself at the concentration of 80 μg/mL against gram-positive bacteria *Staphylococcus aureus* and *Bacillus subtilis,* showed promising antibacterial activity when tested together with antibiotic adjuvant disulfiram. Although disulfiram alone exhibited some antibacterial activity against *S. aureus* [Ejim et al., 2011], CA-MRSA CA-347 [Long, 2017], and HA-MRSA COL [Long, 2017] with MIC values of 32, 16 and 8 μg/mL, respectively, our results showed that when tested against *S. aureus* (ATCC® 12600™) and *Bacillus subtilis* (ATCC®6633™) disulfiram alone was not active at 24 μg/mL. Remarkably, disulfiram also has the ability to enhance the activity of FDA-approved antibiotics [Ejim et al., 2011], indicating that pathogenic bacteria are more susceptible to antibiotic agents in the presence of disulfiram. Our bioassay-guided fractionation using disulfiram as an adjuvant led to the identification of six previously undescribed polyketides (**1–6**). Herein, we report the isolation, structural elucidation by HR-ESIMS, NMR spectral interpretation, and ECD analysis, and the biological evaluation of compounds **1–6** from *Fusarium* sp. FM701.

2. Results and discussion

2.1. Structural elucidation of the previously undescribed compounds

Compound **1** (Fig. 1) was obtained as whitish powder and its molecular formula was determined as $C_{16}H_{20}O_4$ by HRESIMS, requiring 7 degrees of unsaturation. Comprehensive analysis of the ^1H, ^{13}C and HSQC NMR spectra indicated the presence of 16 carbons including four methyl groups (4 × CH_3), six olefinic methines (6 × C=HC) and six non-protonated carbons including two carboxyl groups (2 × -COO-) (Table 1). ^1H–^1H COSY spectrum establishes three spin systems, –C(CH_3) = CH–C=HCH-, –C(CH_3) = CH–C(CH_3) = CH-, and-=CCH–CH_3 (Fig. 2). HMBC correlations (Fig. 2) from H_3-15 to C5, C6 and C7 enabled us to connect the first two spin systems together as –C(CH_3) = CH–C=HCH–C(CH_3) = CH–C(CH_3) = CH-. In the HMBC spectrum of 1, H-9 correlated to C-11 and C-17 (a carbonyl), indicating that these three spin systems formed a 2,6,8,10-tetrasubstituted straight chain with five double bonds at 2-, 4-, 6-, 8, and 10-positions [-C(CH_3) = CH–C=HCH–C(CH_3) = CH–C(CH_3) = CH–C(CO=O)CH–CH_3]. HMBC correlations from H_3-13 to C-1 (a carbonyl), C-2 and C-3 established the flat structure of compound 1 as HOOC–C(CH_3) = CH–C=HCH–C(CH_3) = CH–C(CH_3) = CH–C(COO=H)CH–CH_3. The conjugated double bonds at 2-, 4-, 6-, 8, and 10-positions were determined to be *trans* on the basis of NOESY correlations and comparison of chemical shifts with literature [Vesonder, 1996; Alécio et al., 1998]. Compound **1** is a derivative of 2,4, 5,8,10-dodecapentaenoic acid with a carboxyl group at 10-position and methyl groups at 2-, 6-, and 8-positions [Jaffe et al., 1966]. Hence, the structure of compound **1** was determined as shown, which was given a trivial name kaneoheoic acid A.

The molecular formula of compound **2** (Fig. 1) was determined as $C_{17}H_{24}O_6$ by HR-ESIMS analysis, with 6 degrees of unsaturation. ^1H, ^{13}C and HSQC spectra confirmed 17 carbons in **2** including five methyl (5 × CH_3, including one O–CH_3), one oxygenated methane (1 × CH–O), five olefinic carbons (5 × C=HC), and six non-protonated carbons including one oxygenated carbon and two carboxyl groups (2 × -COO-) (Table 1). The ^1H NMR and HSQC spectra of **2** were similar to those of **1** except 6-, 7-, and 17-positions. Like **1**, COSY spectrum of **2** showed three spin systems, –C(CH_3) = CH–C=HCH-, –C(CH_3)–CH–C(CH_3) = CH-, and-=CCH–CH_3 (Fig. 2). HMBC correlations (Fig. 2) from H_3-15 to C-5, C-6 (oxygenated), and C-7 (oxygenated), and from the oxygenated methyl (O–CH_3) to C-17 indicated that **2** was a derivative of **1** with a diol at 6-/7-positions and a methyl ester at 17-position. The double bonds at 2-, 4-, 8, and 10-positions were determined to be *trans* on the basis of NOESY correlations and comparison of chemical shifts with literature [Vesonder, 1996; Alécio et al., 1998].

To determine the configuration of compound **2**, ECD spectra were collected (Fig. 3). Compound **2** showed a strong negative Cotton effect at 210–220 nm. The calculated weighted ECD spectra of **2***SS* and **2***SR* showed a strong negative Cotton effect at 210–220 nm, coinciding with the experimental ECD spectrum (Fig. 3), which excluded **2***RR* and **2***RS* as the possible structure of **2**. To verify the above analysis, we carried out NMR calculations of **2***SS* and **2***SR* with the conformers generated for ECD calculation. Results showed that the calculated NMR data of **2***SS* matched the experimental NMR data of **1** better than **2***SR*

(Table S1), which enabled final assignment of the absolute configuration of **2** as shown. Compound **2** was given a trivial name kaneoheoic acid B.

Compound **3** (Fig. 1) exhibited a prominent deprotonated molecule peak at *m/z* 241.1433 [M - H]$^-$ in the HR-ESIMS spectrum, suggesting a molecular formula of $C_{13}H_{22}O_4$. ^{1}H NMR and HSQC data (Table 2) defined two methyls (2 × CH_3), four methylenes (4 × CH_2), two oxygenated aliphatic methines (2 × CH–O), three olefinic methines (3 × C=HC), one carbonyl (1 × O–C=O), and one non-protonated carbon. ^{1}H–^{1}H COSY spectrum demonstrated two spin systems –C=HCH- and –C(CH_3) = CH–CH(O)–CH(O)–CH_2–CH_2–CH_2–CH_2–CH_3 (Fig. 4). HMBC correlations from H_3-14 to C-3, C-4, and C-5 connected the two spin systems as –C=HCH–C(CH_3)=CH–CH(O)–CH(O)–CH_2–CH_2–CH_2–CH_2–CH_3. HMBC correlation from H-3 to C-1 (Fig. 4) established the flat structure as HOOC–C=HCH–C(CH3)=CH–CH(OH)–CH(OH)–CH_2–CH_2–CH_2–CH_2–CH_3. The double bonds at 2- and 4-positions were also determined to be *trans*. Compound **3** was structurally similar to 2*E*,4*E*,6*R*-4,6-dimethyl-dodecadienoic acid [Yu et al., 2020], but has 1,2-diol moiety at 6- and 7-position instead of a methyl group at 6-position.

To determine the relative configurations of compound **3**, we next carried out a *J*-based configuration analysis to determine the configuration of 6- and 7-positions. For the 1,2 methine system at C6–7, the $^3J_{H\text{-}6,H\text{-}7}$ (4.9 Hz), $^2J_{H\text{-}6,C\text{-}7}$ (−1.6Hz), $^2J_{H\text{-}7,C\text{-}8}$ (−2.6Hz), and $^3J_{H\text{-}7,C\text{-}5}$ (1.8 Hz) values indicated a *Threo* configuration for compound **3**, which means that it could be **3***RR* or **3***SS* (Fig. 5). To determine the absolute configuration of compound **3**, ECD spectra were collected, and ECD calculations were carried out. Compound **3** showed a strong negative Cotton effect at 210–215 nm, which was similar to the calculated weighted ECD spectra of **3***SS* (Fig. 6). Hence, the structure including the absolute configuration of compound **3** was determined as shown, and it was given a trivial name kaneoheoic acid C.

Compound **4** (Fig. 1) also exhibited a peak at *m/z* 241.1433 [M - H]$^-$ in the HR-ESIMS spectrum, however with a different retention time. The NMR spectra of **4** were almost the same as those of compound **3**. So it is most likely a stereoisomer of compound **3**, which means it is either **4***SR* or **4***RS*. ECD calculations were carried out to determine the absolute configuration of compound **4**, which showed a strong negative Cotton effect at 240–260 nm, coinciding with the calculated weighted ECD spectra of **4***SR* (Fig. 7). Hence, the structure including the absolute configuration of compound **4** was determined as shown, and it was given a trivial name kaneoheoic acid D.

Compound **5** (Fig. 1) is a light brownish powder whose molecular formula was determined to be $C_{13}H_{18}O_3$ from HR-ESIMS. ^{1}H–^{1}H COSY spectrum exhibited three spin systems, –C=HCH-, and –C(CH_3)= CH–C=HCH–CH_2–CH_2-, and –CH_2-CH_3. The double bonds at 2-, 4- and 6-positions were determined to be *trans*. HMBC correlations (Fig. 8) from H_3-14 to C-3, C-4, and C-5, from H_3-12 to C-10 (a carbonyl), and C-11, from H_2-8 to C-10, and from H-3 to C-1 (a carboxyl) connected the three spin systems together, and established the structure as shown. Compound **5** was given a trivial name kaneoheoic acid E.

Compound **6** (Fig. 1) was isolated as light brownish powder, and was determined to have the same molecular formula $C_{13}H_{18}O_3$ as **5** on the basis of HR-ESIMS. However, **6** had a

different retention time, suggesting that **6** was a stereoisomer of compound **5**. The NMR spectra of **6** were very similar to those of **5**. The only difference between compound **5** and compound **6** was the location of the ketone group, which was at 11-position in **6** instead of 10-position in **5**. HMBC correlations from the methyl singlet at 12-position to C-11 (a ketone) and C-10 (Fig. 8) confirmed the location of the double bond. Hence, the structure of compound **6** was determined as shown, and it was given a trivial name kaneoheoic acid F. Compound **6** was an analog of 2*E*,4*E*,6*E*-6-hydroxy-4-methyl-dodecatrienoic acid [Lorenzen et al., 1996], but has a ketone at 11-position instead of a hydroxy group at 11-position.

2.2. Antibacterial and anti-proliferative activity of the kaneoheoic acids (1–6)

All these six previously undescribed compounds (**1–6**) are derivatives of dodecanoic acid (lauric acid) with different functional groups including double bound, hydroxy, methyl, ketone, carboxyl and carboxymethyl ester. It has been reported that lauric acid and its derivatives have antibacterial (Rouse et al., 2005), antifungal (Rihakova et al., 2001), antitumour (Kato et al., 1971), anti-inflammatory (Calder and Grimble, 2002), antimycobacterial (Saravanakumar et al., 2008) and antiviral (Villamor et al., 2007) activities. To test the biological activities of kaneoheoic acids A-F (**1–6**), we evaluated them in our antibacterial and anti-proliferative assays.

Compounds **1–6** were evaluated for their antibacterial activity against *S. aureus, B. subtilis.* and *E. coli*. Although none of them were active by themselves, even at 80 μg/mL, all the compounds showed significant antibacterial activity against *S. aureus* when given with 6 μg/mL disulfiram. In the presence of disulfiram (6 μg/mL), compounds **4** and **5** (MIC 10 μg/mL each) were more potent than compounds **1** and **6** (MIC 20 μg/mL each), which were more active than compounds **2** and **3** (MIC 40 μg/mL each). Moreover compounds **2–6** also showed mild antibacterial activities against *B. subtilis* with MICs ranging from 40 to 80 μg/mL, when tested in the presence of chloramphenicol with half of its MIC value (1 μg/mL) (Table 3 and S2).

To compare our findings with commercially available short, medium, and long chain fatty acids, we also tested five fatty acids such as butyric acid [CH_3-$(CH_2)_2$–COOH], capric acid [CH_3-$(CH_2)_8$–COOH], lauric acid [CH_3-$(CH_2)_{10}$–COOH], myristic acid [CH_3-$(CH_2)_{12}$–COOH] and linoleic acid [$C_{18}H_{32}O_2$, CH_3-$(CH_2)_4$-^{Z}CH=CH–CH_2-^{Z}CH=CH-$(CH_2)_7$-COOH] for their antibacterial properties against *S. aureus* and *B. subtilis* in the presence of disulfiram or chloramphenicol. Although most of them showed very mild antibacterial activity with MIC values ranging from 63 μg/mL to 1.1 mg/mL when tested alone, in almost every case the MIC values decreased 2–4 folds when combined with either disulfiram or chloramphenicol (Table S3). These findings confirmed the synergistic potentials of the newly isolated fatty acids (**1–6**) from *Fusarium* sp. FM701. Although much less potent than compounds **1–6**, lauric acid (a medium chain fatty acid) with twelve carbon atoms like compounds **1–6** was the most active among all the purchased fatty acids. Lauric acid and some other fatty acids have been investigated for their antibacterial activity extensively [Butt et al., 2016; Fisher et al., 2012; Rouse et al., 2005], but lauric acid in combination with disulfiram has not been studied before for its anti-*S. aureus* activity. The results strongly suggested that the lengths of the fatty acids and functional groups in the molecules (for

examples, double bonds, hydroxy groups, and methyl groups) are important for the antibacterial activity.

Compounds **1–6** were further assayed for their anti-proliferative activity (Cao et al., 2010) against A2780 human ovarian cancer cells and HEK293 human embryonic kidney cells, but none was active at 40 μM (the highest concentration tested). The results indicated that non-toxic fatty acids like compounds **1–6** have potential to be antibiotics when used together with the adjuvant disulfiram.

3. Conclusion

In conclusion, six previously undescribed medium chain polyketide-derived fatty acids, kaneoheoic acids A-F (**1–6**) from *Fusarium* sp. FM701 are unique in structure with promising antibacterial potentials against gram-positive pathogenic bacteria. Compared to the other fatty acids, these previously undescribed fatty acids from *Fusarium* sp. FM701 showed significant antibacterial activities against *S. aureus* and *B. subtilis* when screened co-currently with either antibiotic adjuvant disulfiram or the FDA approved antibiotic chloramphenicol. The combination of FDA-approved non-antibiotic drugs (e.g., disulfiram) which acts as antibiotic adjuvant or enhancer with non-toxic fatty acids provides an opportunity to expand a previously untapped bioactive chemical space in the field of antibiotic drug discovery. The findings from the present study warrant future research on the mechanism of action behind these synergistic activities.

4. Experimental

4.1. General experimental procedure

Optical rotations, CD and FT-IR spectra were measured with a Rudolph research analytical autoPol automatic polarimeter, JASCO J-815 CD and Thermo scientific nicolet iS10 IR spectrometer, respectively. 1D and 2D NMR spectra were recorded on a Bruker AM-400 spectrometer. The 3.35 ppm and 49.3 ppm resonances of CD_3OD were used as internal references for ^{1}H and ^{13}C NMR spectra, respectively. An Agilent 6530 accurate-Mass Q-TOF LC-MS spectrometer was used to record high-resolution mass spectra. Preparative HPLC was carried out on an Ultimate 3000 chromatographic system with a Phenomenex preparative column (Phenyl-Hexyl, 5 μm, 100 × 21.2 mm) and semi-preparative HPLC on an Ultimate 3000 chromatographic system with a Phenomenex semi-preparative column (C_8, 5 μm, 250 × 10 mm), a Dionex Ultimate 3000 DAD detector and a Dionex Ultimate 3000 automated fraction collector; and all solvents were HPLC grade. Diaion HP-20 was used to run open column chromatography.

4.2. Strain isolation and fermentation

The strain FM701 was isolated from a muddy sample collected at the Kaneohe Bay, Oahu, Hawaii. The strain was sub-cultured on potato dextrose agar containing 15% marine sea water and maintained at −80 °C in 20% glycerol at Daniel K. Inouye College of Pharmacy, University of Hawaii at Hilo, HI, USA. The frozen strain from −80 °C freezer was activated on PDA plates at 28 °C for 5 days, then it was cut into small pieces and inoculated into 15 L autoclaved sterilized liquid medium [mannitol 20 g, glucose 10 g, monosodium glutamate 5

g, KH_2PO_4 (0.5 g), $MgSO_4 \cdot 7H_2O$ 0.3 g and yeast extract 3 g for 1 L distilled water; pH 6.5 prior sterilization] for fermentation at 24 °C for 28 days in static condition.

4.3. Molecular identification

DNA extraction: DNA was extracted according to the literature (Liu et al., 2000), with slight modifications. Mycelium was added to 500 μl of lysis buffer (400 mM Tris-HCl [pH 8.0], 60 mM EDTA, 150 mM NaCl, 1% sodium dodecyl sulfate) and incubated at 85°C for 20 minutes. After adding 150 μl of 3 M sodium acetate (pH 5.2), the tube was vortexed briefly and centrifuged (12,500 x g) for 1 minute. The supernatant was transferred to another tube and centrifuged again. After transferring the supernatant to a new tube, an equal volume of isopropanol was added and mixed by inversion. The tube was centrifuged for 2 minutes and the supernatant was discarded. The DNA pellet was washed twice with 300 μl of 70% ethanol. The DNA was air dried at room temperature for 45 minutes, then dissolved in 100 μl of 10 mM Tris-HCl (pH 8.0).

Sequencing of ITS region: The ITS region was amplified with the ITS1 and ITS4 primers. The PCR reaction included 1X High Fidelity PCR Buffer (Invitrogen), 2 mM $MgSO_4$, 0.2 mM dNTP mix, 4% DMSO, 0.2 μM of each primer, 1 U Platinum Taq DNA Polymerase High Fidelity (Invitrogen), and 10 ng of genomic DNA. The PCR cycling conditions were 95°C for 3 minutes, followed by 35 cycles of 95°C for 30 seconds, 50°C for 30 seconds and 72°C for 1 minute, and a final extension of 72°C for 5 minutes. The PCR product was purified using Mag-Bind Total Pure NGS beads (Omega Bio-tek), then sequenced using a 3730xl DNA Analyzer (Applied Biosystems). The sequence was compared to the NCBI nucleotide collection (limited to sequences from type material) using the Basic Local Alignment Search Tool (BLAST), and was deposited in GenBank under the accession no. MW130722.

4.4. Extraction and isolation

The mycelia of FM107 were filtered and extracted with acetone under ultrasonic (2 L × 3 times), followed by removal of acetone under reduced pressure to afford an aqueous solution. After combining the aqueous mycelia extract and supernatant solution, it was subjected to HP-20 column eluted with MeOH–H_2O (10, 50, 90 and 100%) to afford four fractions (Fr 1–4). Fraction 3 (12 g) was separated by prep-HPLC (Phenyl-Hexyl, 5 μm, 100 × 21.2 mm; 8 mL/min) eluted with 40–80% MeOH–H_2O in 20 min to yield sub-fractions (SFr 3–1–20). Compound **1** (0.9 mg, t_R 13 min) was separated from SFr 3–13 by using a semi-preparative HPLC (50% isocratic of MeOH–H_2O with 0.1% formic acid for 20 min). SFr 3–10 was purified by using a semi-preparative HPLC (60% isocratic of MeOH–H_2O with 0.1% formic acid for 20 min; 3 mL/min) to afford compounds **2** (1.2 mg, t_R 12 min), **3** (0.8 mg, t_R 17 min), and **4** (1.6 mg, t_R 19 min) while compound **5** (1.8 mg, t_R 16 min) and **6** (2 mg, t_R 19 min) were isolated from SFr 3–8 and SFr 3–9 also by using a semi-preparative HPLC (75% isocratic of MeOH–H_2O with 0.1% formic acid for 20 min; 3 mL/min).

4.5. Spectroscopic data of compounds 1–6

***Kaneoheoic acid A* (1):** White, amorphous powder; $[\alpha]_D^{25}$ 13.4 (*c* 0.2, MeOH); UV (MeOH) λ_{max} (log ε) 340.09 (2.40) nm; IR ν_{max} 3328, 2942, 2834, 1660, 1441, 1401, 1115, 1014 cm^{-1}; ^{1}H and ^{13}C NMR data, Table 1; HRESIMS *m/z* 275.1284 $[M - H]^-$ (calcd for $C_{16}H_{19}O_4$, 275.1283).

***Kaneoheoic acid B* (2):** White, amorphous powder; $[\alpha]_D^{25}$ 17.3 (*c* 0.2, MeOH); UV (MeOH) λ_{max} (log ε) 265.44 (3.10) nm; IR ν_{max} 3328, 2942, 2831, 1447, 1022 cm^{-1}; ^{1}H and ^{13}C NMR data, Table 1; HRESIMS *m/z* 323.1499 $[M - H]^-$ (calcd for $C_{17}H_{23}O_6$, 323.1495).

***Kaneoheoic acid C* (3):** Brownish powder; $[\alpha]_D^{25}$ 18.7 (*c* 0.2, MeOH); UV (MeOH) λ_{max} (log ε) 255.13 (3.41) nm; IR ν_{max} 3315, 2943, 2831, 2043, 1448, 1410, 1115, 1022 cm^{-1}; ^{1}H and ^{13}C NMR data, Table 2; HRESIMS *m/z* 241.1433 $[M - H]^-$ (calcd for $C_{13}H_{21}O_4$, 241.1440).

***Kaneoheoic acid D* (4):** Brownish powder; $[\alpha]_D^{25}$−14.8 (*c* 0.2, MeOH); UV (MeOH) λ_{max} (log ε) 265.64 (2.85) nm; IR ν_{max} 3313, 2898, 2803, 2434, 1632, 1472, 1422, 1121, 1020 cm^{-1}; ^{1}H and ^{13}C NMR data, Table 2; HRESIMS *m/z* 241.1433 $[M - H]^-$ (calcd for $C_{13}H_{21}O_4$, 241.1440).

***Kaneoheoic acid E* (5):** Brownish powder; $[\alpha]_D^{25}$ 17.3 (*c* 0.2, MeOH); UV (MeOH) λ_{max} (log ε) 305.70 (3.28) nm; IR ν_{max} 3312, 2942, 2813, 2358, 1642, 1445, 1412, 1114, 1020 cm^{-1}; ^{1}H and ^{13}C NMR data, Table 2; HRESIMS *m/z* 223.12137 $[M + H]^+$ (calcd for $C_{13}H_{19}O_3$, 223.12895).

***Kaneoheoic acid F* (6):** Brownish powder; $[\alpha]_D^{25}$ 12.2 (*c* 0.2, MeOH); UV (MeOH) λ_{max} (log ε) 305.30 (3.14) nm; IR ν_{max} 3302, 2948, 2824, 2434, 1632, 1445, 1416, 1115, 1017 cm^{-1}; ^{1}H and ^{13}C NMR data, Table 2; HRESIMS *m/z* 223.12690 $[M + H]^+$ (calcd for $C_{13}H_{19}O_3$, 223.12895).

4.6. Computational section [Wang et al., 2018, 2019a, Wang et al., 2019b]

Mixed torsional/low-frequency mode conformational searches were carried out by means of the MacroModel v 11.5 software using the OPLS 2005 with an implicit solvent model for water, retaining the geometries within 5.02 kcal/mol of the global minimum. Geometry re-optimization and frequency calculation were performed with the B3LYP functional with the 6–31+G (d, p) basis set using the Gaussian 09 software. NMR shielding tensors were computed with the GIAO method in Gaussian 09 using the B3LYP functional with the 6–311+G (2d, p) basis set, with methanol as solvent of the integrated equation formalism polarized model (IEFPCM). The unscaled chemical shifts were scaled using regression analysis parameters created by the method of Tantillo et al. [Lodewyk et al., 2011]. and Boltzmann-weighted average shielding tensor data set were calculated thereafter. ECD calculations were performed with the APFD functional with the 6–311+G (2d, p) basis set

with methanol as solvent. The Boltzmann-averaged spectrum was obtained by GaussView 5.0.

4.7. Antibacterial assay

Antibacterial assay was conducted by using the previously described method [Zaman et al., 2020]. Bacteria were grown on agar plates [Tryptic Soy Agar (TSA), Brain heart infusion agar (BHIA) or Luria–Bertani Agar(LBA)] for 1 day at 37 °C and then added to a liquid medium (TSB for *S. aureus*, BHIB for *B. subtilis* and LB for *E. coli*). After incubation at 37 °C for 20 h, the cultures were diluted with TSB, BHIB or LB media to obtain an OD_{600} value of approx. 0.1. One hundred microliter of fresh media with samples at the desired concentration of 80 μg/mL (dissolved in DMSO) was put in the first well and then a two-fold dilution continued to the lowest concentration. The bacterium-containing media (100 μL) were then added to each well of 96-well plates. Additionally, samples were tested in combination with the FDA approved antibiotic chloramphenicol at 1 μg/mL, and two antibiotic adjuvants disulfiram (for *S. aureus* and *Bacillus subtilis*) or Loperamide (for *E. coli*) at 6 μg/mL. DMSO (5%), chloramphenicol (1 μg/mL) and the antibiotic adjuvants (6 μg/mL) were used as negative controls in these sets of experiments. Chloramphenicol, which is active against *S. aureus, Bacillus subtilis* and *E. coli* at MIC values of 6.25 μg/ml, 10 μg/ml and 3.2 μg/ml, respectively, was employed as the a positive control.

Supplementary Material

Refer to Web version on PubMed Central for supplementary material.

Acknowledgement

This work was financially supported by start-up funding from Daniel K. Inouye College of Pharmacy (DKICP), Seed Grants from University of Hawaii at Hilo (UHH), and the Victoria S. and Bradley L. Geist Foundation (15ADVC-74420, 17CON-86295, and 20CON-102163) (to SC). Funding for this work was also supported by Hawaii IDeA Network for Biomedical Research Excellence III and IV (INBRE-III and INBRE-IV) project: NIGMS Grant 5P20GM103466. We would also like to express our gratitude to Mr. Justin Reinicke for his help with NMR and for his kind assistance with optical rotation and ECD data collection.

References

Alécio AC, Bolzani V da Sliva, Young MCM, Kato MJ, Furlan M, 1998 Antifungal amide from leaves of *Piper hispidum*. J. Nat. Prod. 61, 637–639. [PubMed: 9599264]

Aly H, Debbab A, Proksch P, 2011 Fungal endophytes: unique plant inhabitants with great promises. Fungal Divers. 50, 3–19.

Butt U, ElShaer A, Chaidemenou A, Alany RG, Snyder Lori AS, Alany RG, 2016 Fatty acid microemulsion for the treatment of neonatal conjunctivitis: quantification, characterisation and evaluation of antimicrobial activity. Drug Deliv. Transl. Res. 6 (6), 722–734. [PubMed: 27766599]

Calder PC, Grimble RF, 2002 Polyunsaturated fatty acids, inflammation and immunity. Eur. J. Clin. Nutr. 56 (3), S14–S19. [PubMed: 12142955]

Cao S, Brodie PJ, Callmander M, Randrianaivo R, Rakotobe E, Rasamison VE, Kingston DGI, 2010 Saponins and a lignan derivative of Terminalia tropophylla from the Madagascar Dry Forest. Phytochemistry 71, 95–99. [PubMed: 19875137]

Ejim L, Farha MA, Falconer SB, Wildenhain J, Coombes BK, Tyers M, Brown ED, Wright GD, 2011 Combinations of antibiotics and nonantibiotic drugs enhance antimicrobial efficacy. Nat. Chem. Biol. 7, 348–350. [PubMed: 21516114]

Fei-Zhang J, Li C, Cao S, 2016 Hawaii natural compounds are promising to reduce ovarian cancer deaths. Canc. Biol. Ther. 17, 709–712.

Fischer CL, Drake DR, Dawson DV, Blanchette DR, Brogden KA, Wertz PW, 2012 Antibacterial activity of sphingoid bases and fatty acids against gram-positive and gram-negative bacteria quick view other sources. Antimicrob. Agents Chemother. 56 (3), 1157–1161. [PubMed: 22155833]

Fotso J, Leslie JF, Smith JS, 2002 Production of beauvericin, moniliformin, fusaproliferin, and fumonisins B1, B2, and B3 by fifteen ex-type strains of *Fusarium* species. Appl. Environ. Microbiol. 68, 5195–5197. [PubMed: 12324376]

Huang P, Li C, Sarotti AM, Turkson J, Cao S, 2017 Sphaerialactonam, a γ-lactam–isochromanone from the Hawaiian endophytic fungus *Paraphaeosphaeria sp.* FT462. Tetrahedron Lett. 58, 1330–1333.

Jaffe HH, Miller Albert L., 1966 Tautomeric equilibriums. VIII. A direct spectroscopic method quick view other sources. Tetrahedron Lett. 14, 1489–1491.

Kato A, Ando K, Tamura G, Arima K, 1971 Effects of some fatty acid esters on the viability and transplantability of Ehrlich ascites tumor cells. Canc. Res. 31, 501–504.

Li C, Sarotti AM, Wu X, Yang B, Turkson J, Chen Y, Liu Q, Cao S, 2019 An unusual benzoisoquinoline-9-one derivative and other related compounds with antiproliferative activity from Hawaiian endophytic fungus *Peyronellaea* sp. FT431. Molecules 24, e196. [PubMed: 30621059]

Li C, Hu Z, Liu Q, Wu X, Cao S, 2018 Two new tricycloalternarenes from Hawaiian endophytic fungus *Didymella sp.* FT433. Tetrahedron Lett. 59, 3381–3383.

Liu Don, Coloe Sue, Baird Rob, Pedersen John, 2000 Rapid mini-preparation of fungal DNA for PCR. J. Clin. Microbiol. 38 (1), 471. [PubMed: 10681211]

Lodewyk MW, Siebert MR, Tantillo DJ, 2011 Computational prediction of 1H and 13C chemical shifts: a useful tool for natural product, mechanistic, and synthetic organic chemistry. Chem. Rev. 112, 1839–1862. [PubMed: 22091891]

Long TE, 2017 Repurposing thiram and disulfiram as antibacterial agents for multidrug-resistant *Staphylococcus aureus* infections. Antimicrob. Agents Chemother. 61 (9) e00898–17. [PubMed: 28674046]

Lorenzen K, Anke T, Sterner O, 1996 11-Hydroxy-4-methyl-2,4,6-dodecatrienoic acid from fermentations of a mucor species quick view other sources. Phytochemistry 43 (4), 791–792. [PubMed: 8987703]

Manzoni M, Rollini M, 2002 Biosynthesis and biotechnological production of statins by filamentous fungi and application of these cholesterol-lowering drugs. Appl. Microbiol. Biotechnol. 58, 555–564. [PubMed: 11956737]

Rihakova Z, Plockova M, Filip V, Smidrkal J, 2001 Antifungal activity of lauric acid derivatives against Aspergillus Niger. Eur. Food. Re.s Technol. 213, 488–490.

Rouse MS, Rotger M, Piper KE, Steckelberg JM, Scholz M, Andrews J, Patel R, 2005 In vitro and in vivo evaluations of the activities of lauric acid monoester formulations against Staphylococcus aureus. Antimicrob. Agents Chemother. 49, 3187–3191. [PubMed: 16048923]

Saravanakumar DEM, Folb PI, Campbell BW, Smith P, 2008 Antimycobacterial activity of the red alga Polysiphonia virgata. Pharm. Biol. 46 (4), 254–260.

Song Q, Nan Z, Gao K, Song H, Tian P, Zhang X, Li C, Xu W, Li X, 2015 Antifungal, phytotoxic, and cytotoxic activities of metabolites from *epichloë bromicola*, a fungus obtained from *Elymus tangutorum* grass. J. Agric. Food Chem. 63, 8787–8792. [PubMed: 26395226]

Vesonder RF, 1996 (all trans)-2,4,6,8,10,12-Tetradecahexene-1,14-dial, a New Pigment from *Conidiobolus paulus*. J. Nat. Prod. 59, 441–442. [PubMed: 8699189]

Villamor E, Koulinska IN, Furtado J, Baylin A, Aboud S, Manji K, Campos H, Fawzi WW, 2007 Long chain n-6 polyunsaturated fatty acids in breast milk decrease the risk of HIV transmission through breastfeeding. Am. J. Clin. Nutr. 86 (3), 682–689. [PubMed: 17823433]

Wang Q, Hu Z, Luo X, Liu J, Li G, Cao S, Liu Q, 2019b Clavukoellians A–F, highly rearranged nardosinane sesquiterpenoids with antiangiogenic activity from *clavulariakoellikeri*. J. Nat. Prod. 82, 1331–1337. [PubMed: 30994348]

Wang C, Wu X, Bai H, Zaman KAU, Hou S, Saito J, Wongwiwatthananukit S, Kim KS, Cao S, 2020 Antibacterial and NF-κB inhibitory lumazine peptides, aspochalasin, γ-butyrolactone derivatives, and cyclic peptides from a Hawaiian Aspergillus flavipes. J. Nat. Prod. 83 (7), 2233–2240. [PubMed: 32568536]

Wang F, Hu Z, Li C, Wu X, Cao S, 2019a Circumdatin M, a new benzodiazepine alkaloid with a unique pyrimidone-4-pyrone moiety from a Hawaiian marine fungus *Aspergillus sp.* FM242. Tetrahedron Lett. 60, 1724–1726.

Wang Q, Hu Z, Li X, Wang A, Wu H, Liu J, Cao S, 2018 Q. Liu, salviachinensines A–F, antiproliferative phenolic derivatives from the Chinese medicinal plant *Salvia chinensis*. J. Nat. Prod. 81, 2531–2538. [PubMed: 30370766]

Yu H, Tian Y, Zong Y, Zhang J, Xu Tao, 2020 Total synthesis and structural reassignment of aranorosinol A, aranorosinol B, and EI-2128–1 quick view other sources. J. Org. Chem. 85 (6), 4335–4343. [PubMed: 32077282]

Zaman KA, Wu X, Hu Z, Hou S, Saito J, Kondratyuk TP, Pezzuto JM, Cao S, 2020 NF-κB inhibitory and antibacterial helvolic and fumagillin derivatives from *Aspergillus terreus*. J. Nat. Prod. 83 (3), 730–737. [PubMed: 32163285]

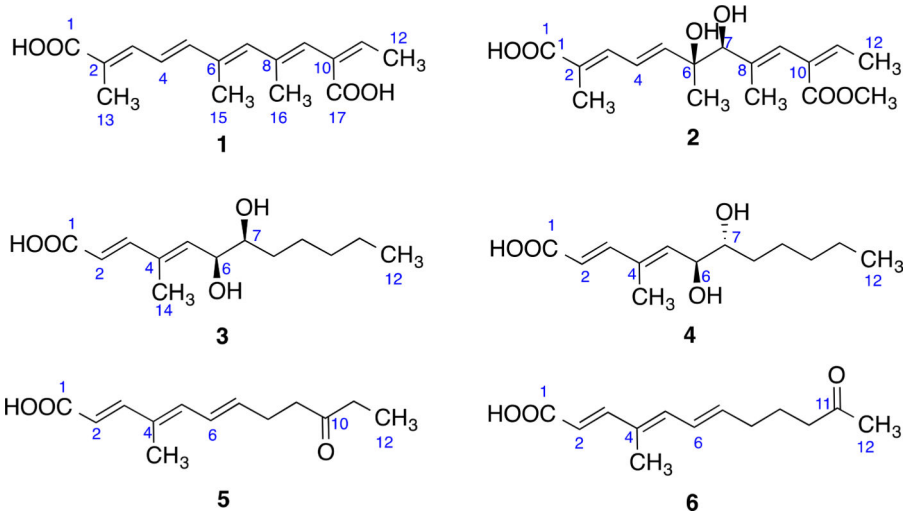

Fig. 1.
Chemical structures of compounds **1–6**.

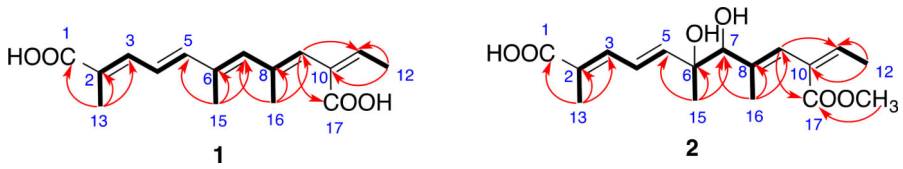

1 **2**

Fig. 2.

Key COSY (bolds) and HMBC (red arrows) correlations of compounds **1** and **2**.

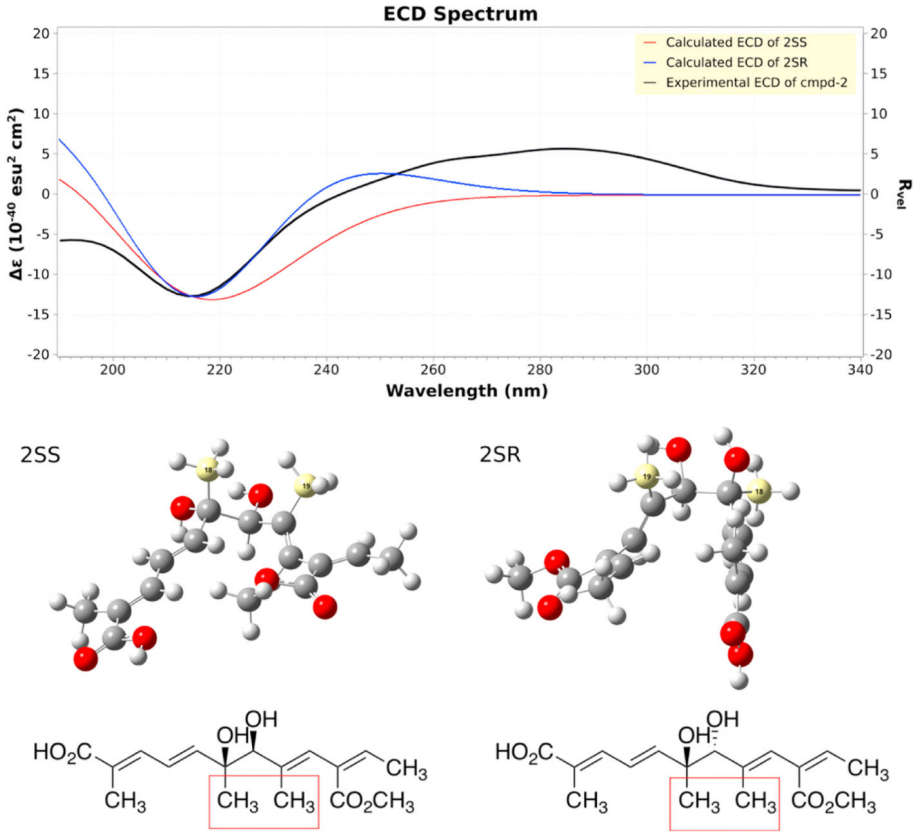

Fig. 3.
Experimental and calculated ECD of compound **2**.

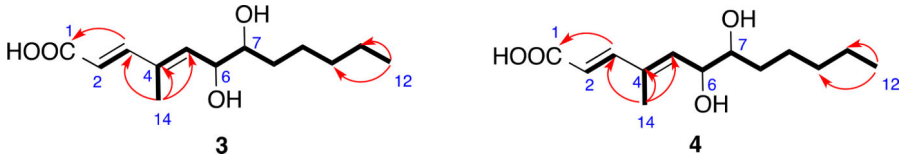

Fig. 4.
Key COSY (bolds) and HMBC (red arrows) correlations of compounds **3** and **4**.

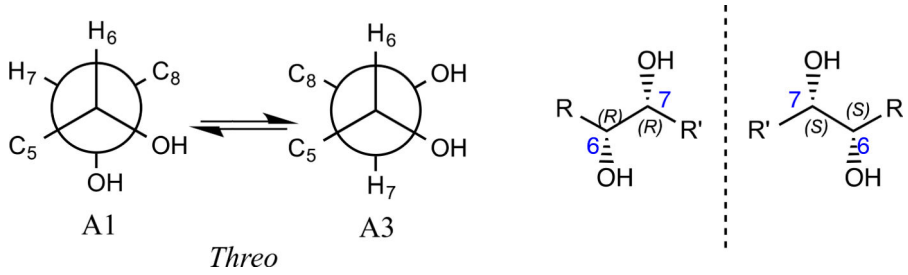

Fig. 5.

J-based configuration analysis of compound **3**.

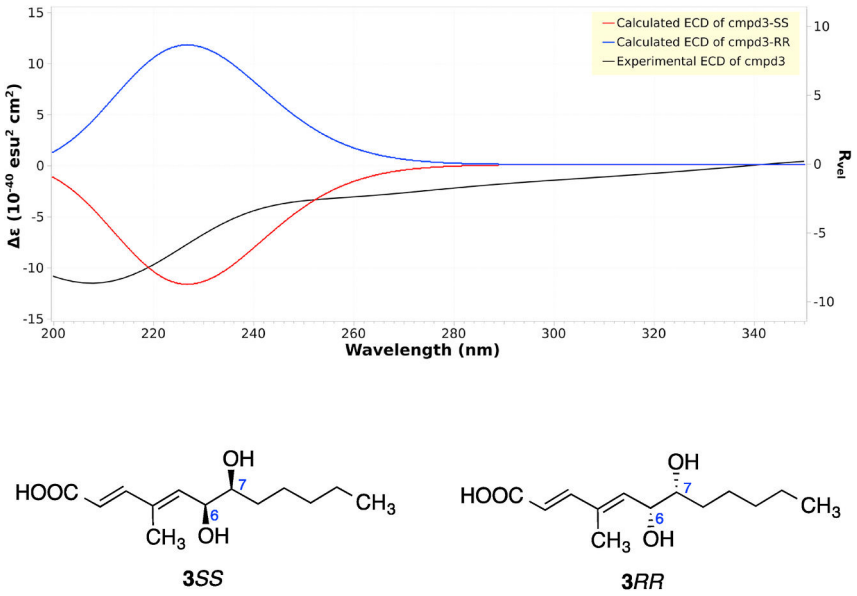

Fig. 6.

Experimental and calculated ECD of compound **3**.

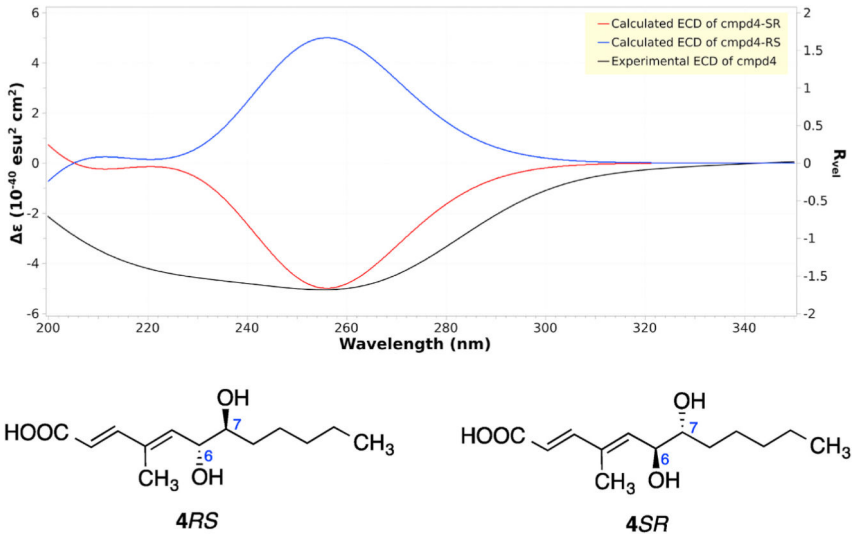

Fig. 7.

Experimental and calculated ECD of compound **4**.

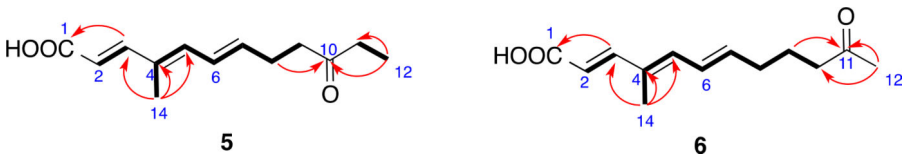

Fig. 8.
Key COSY (bolds) and HMBC (red arrows) correlations of compounds **5** and **6**.

Table 1

^{1}H and ^{13}C NMR spectroscopic data for compounds **1** and **2** in CD_3OD.

no.	1		2	
	δ_C	δ_H mult. *J (Hz)*	δ_C	δ_H multi. *J* (Hz)
1	171.3		171.1	
2	126.9		126.6	
3	137.8	7.28 d (10.6)	137.0	7.23d (11.4)
4	122.6	6.63 t dd (11.3, 15.2)	138.8	6.70 dd (11.3, 15.2)
5	144.0	6.66d (15.1)	145.7	6.25 d (15.2)
6	134.5		75.2	
7	137.6	6.26 s	81.7	4.06 s
8	136.3		141.0	
9	125.7	6.11 s	120.7	5.99 s
10	132.9		130.1	
11	136.3	6.86 m	138.8	6.94 m
12	14.3	1.79 d (7.2)	14.2	1.76 d (7.1)
13	11.4	1.99 s	11.2	1.95 s
15	12.75	2.11 s	23.5	1.36 s
16	17.5	1.76 s	14.1	1.59 s
17	170.9		168.0	
19			50.4	3.73 s

Table 2

NMR spectroscopic data for compounds **3–6** in CD_3OD.

no.	3		4		5		6	
	δ_C	δ_H multi. *J* (Hz)	δ_C	δ_H multi. *J* (Hz)	δ_C	δ_H multi. *J* (Hz)	δ_C	δ_H multi. *J* (Hz)
1	170.1		170.1		170.1		170.7	
2	120.7	5.96 d (15.6)	120.7	5.96 d (15.6)	117.3	5.86 d (15.6)	117.3	5.86 d (15.5)
3	146.4	7.25 d (15.5)	147.8	7.27 d (15.5)	148.9	7.30 d (15.5)	148.3	7.30 d (15.4)
4	135.9		134.7		131.4		132.3	
5	137.4	5.88 d (8.9)	138.5	5.85 d (9.0)	138.3	6.41 d (11.3)	137.5	6.38 d (11.1)
6	70.9	4.33 dd (5.1, 8.9)	70.9	4.30 dd (5.9, 9.0)	127.0	6.51 t (11.9)	126.9	6.51 t (13.0)
7	74.2	3.55 m	74.3	3.48 m	139.3	5.97 m	137.7	5.97 m
8	32.3	1.55 m	32.3	1.38 m 1.50 m	32.4	2.20 m	27.0	2.46 m
9	25.2	1.35 m 1.55 m	25.2	1.36 m 1.51 m	22.9	1.70 m	40.9	2.62 t (7.2)
10	31.7	1.33 m	31.6	1.33 m	42.4	2.53 t (7.3)	212.3	
11	22.3	1.34 m	22.2	1.34 m	210		35.3	2.50 m
12	13.0	0.92 t (6.6)	13.0	0.94 t (6.8)	28.7	2.14 s	6.77	1.05 t (7.3)
14	11.8	1.88 s	11.8	1.90 s	11.4	1.90 s	11.4	1.90 s

Table 3

Activities of compounds **1–6** against *S. aureus* (ATCC® 12600™) and *B. subtilis* (ATCC®6633™) in the presence of disulfiram (6 μg/mL) or chloramphenicol (1 μg/mL).

Compound	MIC [μg/mL]			
	S. aureus		B. subtilis	
	Compound alone	Compound + Disulfiram [6 μg/mL]	Compound alone	Compound + Chloramphenicol [1 μg/mL]
1	NA	20	NA	NA
2	NA	40	NA	80
3	NA	40	NA	40
4	NA	10	NA	80
5	NA	10	NA	80
6	NA	20	NA	40

NA→ Not Active.